Phase Behavior of Aqueous Mixtures of Cetyltrimethylammonium Bromide (CTAB) and Sodium Octyl Sulfate (SOS)

Michael T. Yatcilla,[†] Kathleen L. Herrington,[‡] Laura L. Brasher, and Eric W. Kaler*

Center for Molecular and Engineering Thermodynamics, Department of Chemical Engineering, University of Delaware, Newark, Delaware 19716

Shivkumar Chiruvolu[§] and Joseph A. Zasadzinski

Departments of Chemical and Nuclear Engineering and Materials Engineering, University of California, Santa Barbara, Santa Barbara, California 93106

Received: August 21, 1995; In Final Form: January 19, 1996[⊗]

The phase behavior and aggregate morphology of mixtures of the oppositely charged surfactants cetyltrimethylammonium bromide (CTAB) and sodium octyl sulfate (SOS) are explored with cryotransmission electron microscopy, quasielastic light scattering, and surface tensiometry. Differences in the lengths of the two hydrophobic chains stabilize vesicles relative to other microstructures (e.g., liquid crystalline and precipitate phases), and vesicles form spontaneously over a wide range of compositions in both CTAB-rich and SOS-rich solutions. Bilayer properties of the vesicles depend on the ratio of CTAB to SOS, with CTAB-rich bilayers stiffer than SOS-rich ones. We observe two modes of microstructural transition between micelles and vesicles. The first transition, between rodlike micelles and vesicles, is first order, and so there is macroscopic phase separation. This transition occurs in CTAB-rich solutions and in SOS-rich solutions at higher surfactant concentrations. In the second transition mode, mixtures rich in SOS at low surfactant concentrations exhibit no phase separation. Instead, small micelles abruptly transform into vesicles over a narrow range of surfactant concentration. Since the vesicles that form in mixtures of oppositely charged surfactants are equilibrium microstructures, the microstructural evolution is related solely to the phase transition and is thus under thermodynamic control. This differs from experiments reported on the dissolution of metastable vesicles, such as the detergent solubilization of biological phospholipid membranes, which may be controlled by kinetics. Despite these differences, we find that the evolution in microstructure in our mixtures of oppositely charged surfactants is analogous to that reported for biological membrane solubilization.

Introduction

Aqueous mixtures of oppositely charged surfactants exhibit interesting phase behavior and properties. We have found that vesicles form spontaneously when oppositely charged surfactants are mixed in aqueous solution. To tailor microstructure and solution properties for successful application of these mixtures, it is important to understand how the solution composition and molecular architecture of the surfactants influence the resulting microstructure and phase behavior. In particular, we seek to identify the conditions that favor formation of equilibrium vesicles and how to tailor the size and surface charge density of these vesicles. For example, branching in the surfactant tail appears to stabilize vesicles with respect to the formation of lamellar phases or precipitate. This is evidenced by formation of vesicles over five decades of surfactant concentration in mixtures of cetyltrimethylammonium tosylate (CTAT) with sodium dodecylbenzenesulfonate (SDBS).[1,2] On the other hand, lamellar liquid crystals or a crystalline precipitate forms when surfactants with linear alkyl chains of the same length are mixed.[3,4] In the latter case, vesicles are present only in a narrow range of concentrations, and the vesicles that do form are large (>200 nm) and highly polydisperse.

The microstructural evolution of the spherical micelles (characteristic of aqueous solutions of each pure surfactant) into vesicles as surfactant of opposite charge is added is of considerable interest. There is a vast literature describing the course of vesicle/micelle transitions in mixtures of lipids and detergents of biological utility.[5−9] Structures similar to those found in biological phospholipid systems form in mixtures of oppositely charged synthetic surfactants.[2,4,10,11] Common to both biological systems and synthetic surfactant mixtures are cases where strong growth of long (several micrometers) rodlike micelles occurs between vesicular and micellar phases. For the mixtures of oppositely charged surfactants, this occurs as the mixture composition becomes more neutral. In these cases, samples at compositions intermediate to the micellar and vesicle phases separate into two macroscopic phases.[4,10] In other cases, no macroscopic phase separation is observed,[3] and micelles and vesicles coexist in a single phase. Thus, mixtures of oppositely charged surfactants can be used as models of biological systems to identify the role that various factors play in determining the relationship between solution conditions and the resulting microstructural evolution.

Here we explore the phase behavior and morphology of mixtures of surfactants with highly asymmetric chain lengths: cetyltrimethylammonium bromide (CTAB) and sodium octyl sulfate (SOS). The complementary techniques of quasielastic light scattering (QLS) and cryotransmission electron microscopy (cryo-TEM) are used to probe microstructural evolution of mixed micelles into vesicles along a dilution path.

Materials and Methods

CTAB, obtained from Kodak Chemicals, was recrystallized from a 1/1 mixture of ethanol and acetone. HPLC grade SOS was obtained from Kodak and treated for surface-active impurities[12] using a SEP-Pak C18 cartridge (Waters Assoc., Milford,

* Author to whom correspondence should be addressed.
[†] Current address: Department of Chemical Engineering, Stanford University, Stanford, CA 94305-5025.
[‡] Current address: W. L. Gore and Associates, Inc., 297 Blue Ball Rd., Elkton, MD 21921.
[§] Current address: Department of Chemical Engineering and Materials Science, 151 Amundson Hall, University of Minnesota, Minneapolis, MN 55455.
[⊗] Abstract published in *Advance ACS Abstracts,* March 1, 1996.

0022-3654/96/20100-5874$12.00/0

MA). The SOS concentration following this treatment was determined using a two-phase titration with standardized Hyamine 1622.[13] Samples were prepared by first making stock solutions of either cationic or anionic surfactant at the desired concentration in distilled deionized water. Stock solutions of each pure surfactant were equilibrated at room temperature and filtered through a 0.2 μm filter prior to preparing samples. Samples were prepared by mixing the stock solutions at the desired ratio, and compositions reported are on a weight percent basis. After brief vortex mixing, the solutions were not subjected to any type of mechanical agitation. All samples were equilibrated at 25 °C in a thermostated bath for many months.

Surface tension was measured using a thermostated Krüss Wilhelmy plate tensiometer. Since the cationic surfactant is preferentially adsorbed on glass,[1] surfactant adsorption alters the bulk composition. Thus, dilute samples for tensiometry were prepared in dishes pretreated with multiple rinses of a solution at the desired concentration and maintained at 25 °C. Reproducible results were obtained if the glassware was rinsed three or more times.

Quasielastic light scattering (QLS) measurements were made with a spectrometer of standard design (Brookhaven Model BI-200SM goniometer and Model BI-9000AT correlator) and a Lexel 300 mW Ar laser. All measurements were made at a scattering angle of 90°, and the intensity autocorrelation function was analyzed by the method of cumulants.[14]

Specimens for cryo-TEM were prepared in the controlled environment vitrification system (CEVS) described in detail by Bellare.[15] Specimens of the microstructured liquid are prepared by placing a 3−5 μL drop of the sample on the surface of a holey carbon film (Lacey-substrate, made by Ted Pella, Redding, CA), which was held by a pair of self-locking tweezers mounted on a spring-loaded shaft inside the environmental chamber. Thin liquid films, spanning the holes on the film and ranging from 50 to 500 nm in thickness, were then formed by gently blotting away excess liquid on the grid by touching it with a filter paper. The films were vitrified by plunging the grid into a vial of liquid propane or ethane, held at its freezing point by a surrounding pool of liquid nitrogen. Later, the grid was transferred under liquid nitrogen onto the tip of a Gatan Model 626 cold-stage. Specimens were held at −168 °C and imaged at 100 kV in a Model 2000 FX JEOL transmission electron microscope under low electron doses. Electron images were recorded on SO-163 plates at under-focus conditions and were later developed for 12 min using full-strength D-19 developer (Kodak).

Results

The CTAB/SOS/water phase diagram (Figure 1) represents the results of observations of more than 250 samples made over the course of many months. When samples are initially prepared, vesicles often form over a wide range of compositions. However, as the samples age, the range of compositions that yield vesicles shrinks considerably, particularly at the lamellar phase boundary. Small amounts of the lamellar phase form in two-phase samples close to the vesicle phase and become visible only after aging for days or weeks. Boundaries are assigned only when the visual appearance does not change with time. Note that aqueous mixtures of cationic (R^+X^-) and anionic surfactants (R^-X^+) are actually five-component systems in the sense of the Gibbs phase rule: R^+X^-, R^-X^+, R^+R^-, X^+X^-, and water. Therefore, the pseudoternary phase diagram for R^+X^-, R^-X^+, and water represents only a portion of the phase prism. The full prism is needed to represent compositions in multiphase regions when the surfactant ion and associated counterion separate into different phases, as is the case when precipitate forms.

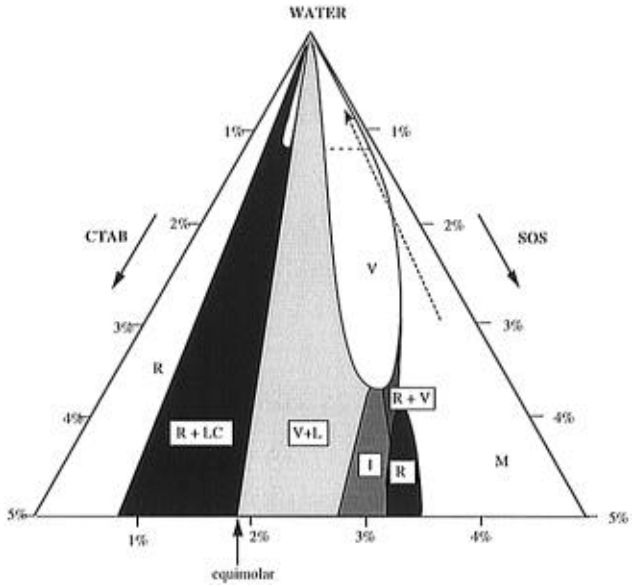

Figure 1. Ternary phase diagram for CTAB/SOS/H_2O at 25 °C. One-phase regions are unshaded and represent SOS-rich vesicles (V), rodlike micelles (R), and SOS-rich micelles (M). Two-phase regions are shaded and are CTAB-rich rodlike micelles and vesicles (R + V), SOS-rich rodlike micelles and vesicles (R + V), SOS-rich vesicles and lamellar phases (V + L_α), and an isotropic liquid and precipitate along the equimolar line. Very small amounts of turbid clouds form in samples in the SOS-rich vesicle lobe with compositions above the horizontal dashed line. Precipitate also forms at low concentrations (up to 0.1 wt %). There is also an unresolved multiphase region (I). The dashed arrow represents the dilution path represented in Figure 3. Compositions are on a weight percent basis.

Micellar phases exist on the binary surfactant−water axes of Figure 1. Vesicles form in the water-rich corner of the phase diagram and are found in both CTAB-rich and SOS-rich samples. Samples with a bluish appearance are designated as containing vesicles, and the presence of vesicles is confirmed by QLS and TEM, as discussed below. The CTAB-rich vesicle lobe is small and narrow in extent, while the SOS-rich vesicle lobe is considerably larger. Micelles form along the binary surfactant−water axes. As SOS is added to CTAB-rich micellar solutions, there is strong rodlike micellar growth, as indicated by increased viscosity and viscoelasticity. Samples become increasingly more viscoelastic at high surfactant concentrations. SOS-rich micelles are spherical at low amounts of added CTAB, while at higher ratios of CTAB to SOS and higher concentrations, rodlike micelles form.

The micelle-to-vesicle phase transition is of considerable interest. For CTAB-rich samples and SOS-rich samples at higher surfactant concentration, there is an intervening two-phase region of rodlike micelles and vesicles. Samples separate into two phases: one phase scatters more light than a micellar solution and is viscous, while the other phase is not viscous. Depending on the composition, the appearance of the second phase ranges from clear and colorless to bluish and somewhat turbid. At higher surfactant concentrations, samples contain more than two phases and may contain vesicles, rodlike micelles, and liquid crystalline microstructures. SOS-rich samples exhibit different behavior for low surfactant concentrations (see Figure 1). In these samples there is limited micellar growth with added CTAB or increased dilution, and the colorless micellar solutions progressively scatter more light than micellar solutions of pure SOS as the micellar phase boundary is approached. Samples become noticeably turbid over a very narrow increment of concentration, and the phase boundary between micelles and vesicles is set at the point at which samples appeared turbid.

For SOS-rich samples with mixing ratios (given as weight of CTAB to weight SOS) between 60/40 and 35/65 CTAB/

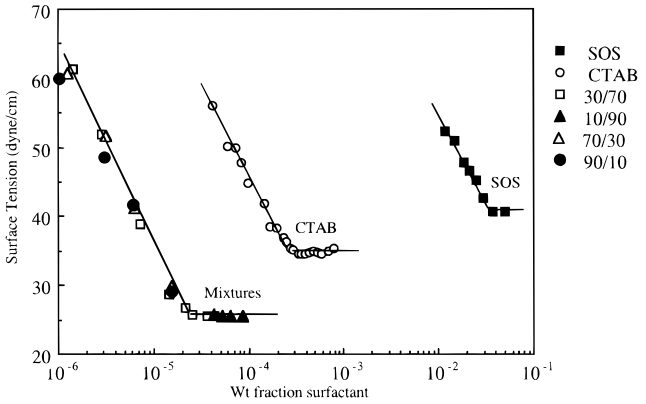

Figure 2. Surface tension of aqueous solutions of pure and mixed surfactants at 25 °C. The break in the surface tension curve represents the onset of aggregation (critical aggregation concentration, cac). The cac for pure SOS is 2 orders of magnitude higher than that of pure CTAB and 3 orders of magnitude higher than that of the mixtures. The cac for all measured mixing ratios falls in roughly the same range (35−70 μM). The mixtures of surfactants show a lower ultimate surface tension value (∼25 dyn/cm) than either of the two pure surfactants (CTAB ∼ 35 dyn/cm; SOS ∼ 40 dyn/cm). Lines are shown to guide the eye.

SOS, the SOS-rich vesicle phase is in equilibrium with a lamellar liquid crystalline phase. At higher SOS concentrations in the multiphase region, solutions appear bluish and are viscoelastic at low concentrations and turbid and birefringent at higher concentrations. Some samples in this region become nonhomogeneous with time, and it is likely that these samples are kinetically trapped multiphase samples.

A crystalline precipitate, presumably the equimolar salt CTA^+:OS^-, forms in equimolar mixtures as well as in dilute (<0.1−0.2 wt %) solutions at all mixing ratios investigated, as indicated in Figure 1. Dilute samples in the vesicle phase close to the precipitate phase boundary often contain turbid wisps that are so easily dispersed by mixing that attempts to characterize them with optical microscopy are unsuccessful. Because of the proximity of the precipitate phase boundary, the wisps may be a fine precipitate or a dilute dispersion of multilamellar vesicles (MLVs).

The critical aggregation concentration (cac) for a variety of mixing ratios, calculated from the break in a plot of surface tension versus the logarithm of the concentration, is shown in Figure 2. The critical micelle concentration (cmc) of pure SOS is approximately 3 wt % (120 mM), and that of pure CTAB is approximately 0.03 wt % (0.88 mM), in agreement with literature values. The critical aggregation concentrations (cac's) for mixtures of CTAB and SOS are significantly lower and range from 0.001 to 0.002 wt % ($(3-7) \times 10^{-5}$ M). Mixtures of CTAB and SOS produce a lower surface tension than is observed for either pure surfactant. Precipitate appears in samples in the vicinity of the cac after equilibration for several days, thus the cac for mixtures of CTAB and SOS corresponds to the solubility of the equimolar precipitate. The value of the solubility product $[=(a_{CTA}+)(a_{SOS}-)]$ for this salt, calculated from the dependence of the cac on bulk mixing ratio, is 9×10^{-10} mol^2 L^{-2}.

To study the transition from micelles to vesicles for SOS-rich mixtures, the apparent aggregate size was measured using QLS along several dilution paths. Figure 3 shows the apparent aggregate radius as a function of surfactant concentration for a mixing ratio of 10/90 CTAB to SOS. There is a gradual increase in aggregate size as the phase boundary is approached, with apparent radii considerably greater than those corresponding to spherical micelles. Below 1.8 wt % surfactant, there is a sharp increase in aggregate size, accompanied by an increase in sample turbidity. This transition occurs at a composition in good agreement with the experimental micelle/vesicle phase boundary shown in Figure 1. The apparent radii of the vesicles range from 100 to 150 nm.

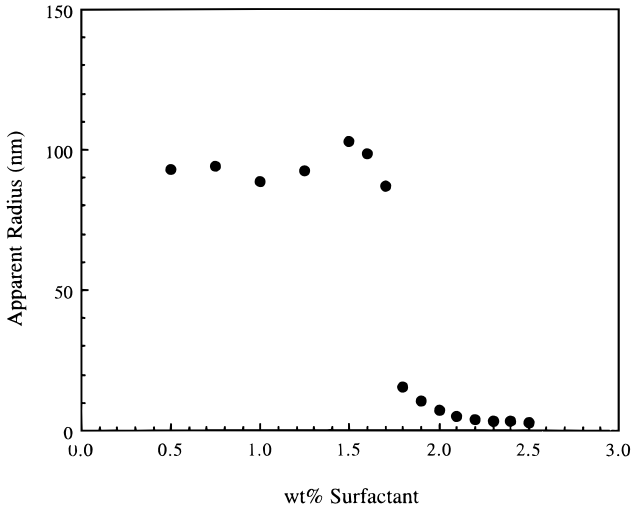

Figure 3. Apparent aggregate radius as a function of surfactant concentration along a dilution path for mixtures of CTAB and SOS. The bulk mixing ratio is 10/90 CTAB to SOS. Apparent radius is measured using QLS 1 month after samples were prepared.

TABLE 1: QLS Results for Mixtures of CTAB and SOS, Measured Immediately Following Preparation and after Aging Several Months

		initial preparation		aged preparation	
mixing ratio	surfactant (wt %)	radius (nm)	polydispersity	radius (nm)	polydispersity
10/90	1.7	19	0.09	158	0.24
	1.4	18	0.08	134	0.26
	1.2	16	0.06	91	0.25
20/80	2.5	36	0.16	74	0.17
	2.0	19	0.13	161	0.30
	1.5	17	0.12	129	0.26
30/70	2.0	35	0.16	136	0.25

The time scale for the transition from micelles to vesicles is very different from that of the reverse transition from vesicles to micelles. To form vesicles, micellar solutions at the desired mixing ratio are diluted with water and vortex-mixed. The samples attain their equilibrium size very slowly, with the apparent radii increasing rapidly in the first hour and much more slowly over the next three months. In contrast, the reverse transition occurs rapidly and the equilibrium micellar size is established within seconds. These results highlight the importance of properly aging vesicle solutions prior to determining properties such as size and polydispersity.

The evolution of apparent radius with time was followed with QLS. Samples were prepared by diluting micellar stock solutions at the desired mixing ratio to the target surfactant concentrations. The results for samples prepared close to the micelle/vesicle phase boundary (mixing ratio of 10/90 CTAB to SOS and total surfactant concentrations of 1.7, 1.4, and 1.2 wt %) and well within the vesicle phase (mixing ratio of 30/70 CTAB to SOS and 2.0 wt % surfactant, and mixing ratio of 20/80 and 1.5, 2.0, and 2.5 wt % surfactant) are shown in Table 1. Initially, all three samples prepared at a mixing ratio of 10/90 CTAB to SOS have approximately the same apparent radius of 16−19 nm. After aging for several months, the sizes increase substantially, as shown in Table 1, with apparent radius inversely proportional to the surfactant concentration. Polydispersity increases significantly, and the signal-to-noise ratio is halved. Turbid clouds that are easily dispersed are occasionally observed in these samples. The behavior of samples

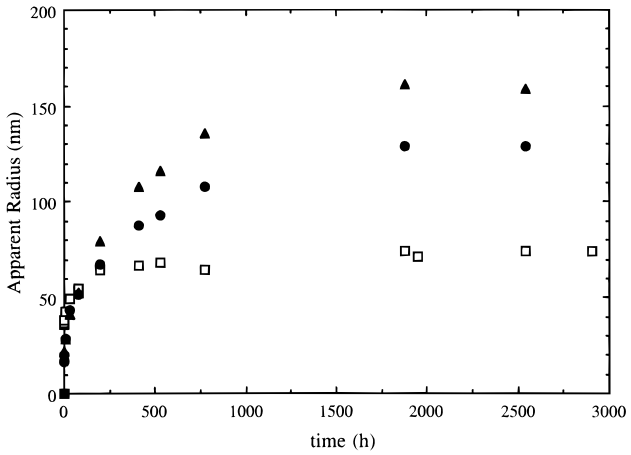

Figure 4. Apparent aggregate radius with time for mixtures of CTAB to SOS. Micellar stock solutions with mixing ratio 20/80 CTAB to SOS are diluted to 2.5 wt % (□), 2.0 wt % (▲), and 1.5 wt % (●) surfactant, which are concentrations within the vesicle lobe. The apparent radius is measured with QLS. After 3 months, apparent radius becomes constant for all three final concentrations for 20/80 CTAB to SOS, indicating that vesicles are equilibrium structures at these compositions.

prepared at these 10/90 compositions near the micelle/vesicle phase boundary is very different from those prepared at the composition ratios of 20/80 or 30/70, which are well within the vesicle lobe. The radius of the latter samples increases rapidly in the first hour after sample preparation and attains an equilibrium size within 3 months (Figure 4). The polydispersity and signal-to-noise ratio also remain constant with time for these samples.

It is well-known that alkyl sulfate surfactants are subject to degradation by hydrolysis of the sulfate head group to the corresponding long chain alcohol.[16] Because of the long equilibration times required to properly determine the phase behavior, we investigated the effect of small amounts of added octanol on phase behavior and vesicle properties. A dilution series at a mixing ratio of 10/90 CTAB to SOS was prepared in which octanol replaced 0.20% of the SOS. Samples containing octanol with compositions in the transition region appear cloudy rather than clear and bluish, and with time, a turbid phase appears in the samples. Thus, the phase behavior of samples with added octanol is different from that of the undoped samples. The apparent radius of aggregates in samples containing added octanol is similar to that of aggregates forming without octanol; however, the octanol-containing structures initially have a much higher polydispersity. The presence of octanol does not significantly affect the concentration at which the increase in apparent radius is observed upon dilution of a micellar solution.

The SOS used in this work was carefully purified to remove surface-active impurities and was shown to be free of octanol by the absence of a minimum in a plot of surface tension versus concentration. We also investigated with NMR the possibility that octanol was forming during aging. SOS samples (1.0 wt %) were aged for 4 months, both at room temperature and under refrigeration. In NMR measurements, no trace of octanol was detected in any of the aged SOS samples. Instrument resolution set the lowest detectable octanol concentration at 0.001 wt %. All of these results show sulfate hydrolysis is not the cause of the observed long-term changes in aggregate morphology.

The microstructure present in samples prepared along the dilution path studied by QLS (10/90 CTAB to SOS and 2.0−0.5 wt % total surfactant) was also probed with cryo-TEM. As expected, micrographs prepared from samples with 2.0−1.8 wt % surfactant, which contain aggregates of hydrodynamic

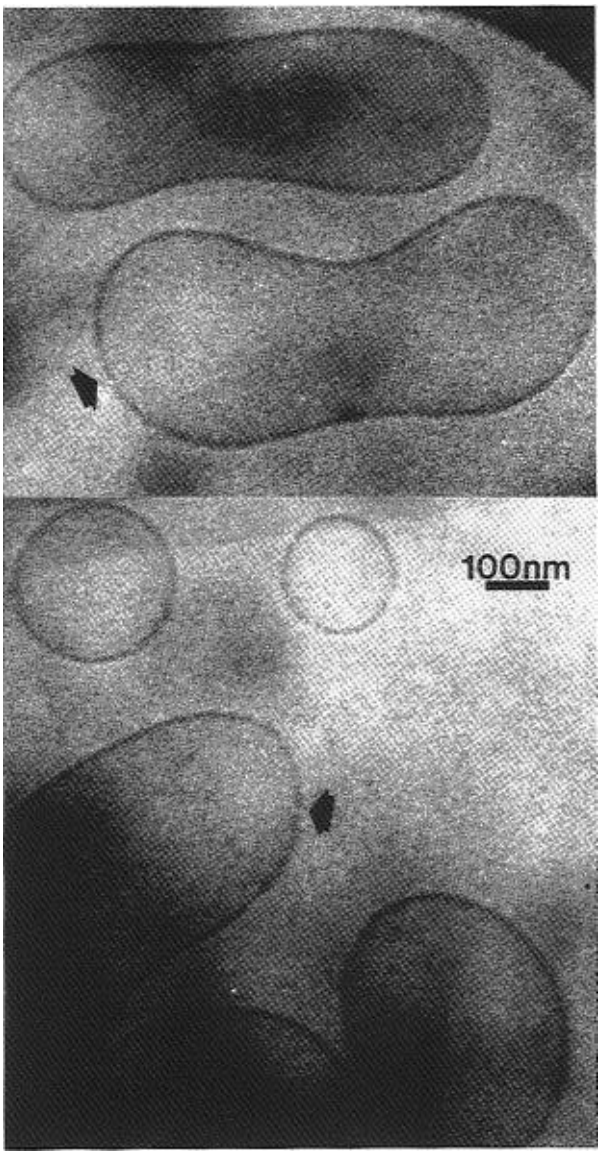

Figure 5. Cryoelectron micrograph of unilamellar vesicles from the vesicle phase at 0.5 wt % surfactant and 10/90 CTAB to SOS. Samples prepared from this solution did not show micelles but only unilamellar vesicles.

radius less than 20 nm and appear clear to the eye, did not show any large aggregates such as vesicles or elongated rodlike micelles. The surfactant in these solutions appears to aggregate only as small (<200 Å) globular or spherical micelles. Electron micrographs (not shown) prepared from solutions containing 0.75−1.8 wt % total surfactant show similar dotted features, and larger aggregates are not observed. Although, it is impossible to identify individual spherical micelles from cryo-electron micrographs, the speckled pattern appears only in samples prepared from such micellar solutions and not in micrographs of deionized water.

Micrographs prepared from samples containing 0.75−1.7 wt % total surfactant show similar features, and larger aggregates are not observed. This is curious since these samples appear bluish to the eye, are slightly turbid at lower surfactant concentrations, and show large sizes by QLS. Thus, images of large aggregates are expected in the micrographs. Although specimens for cryo-TEM were prepared with great care to avoid the exclusion of larger aggregates from the sample, there is likely only a low number density of large aggregates in these samples, and thus they are not captured. Vinson *et al.*[9] reported similar findings.

Vesicles are imaged in the more dilute samples, and Figure

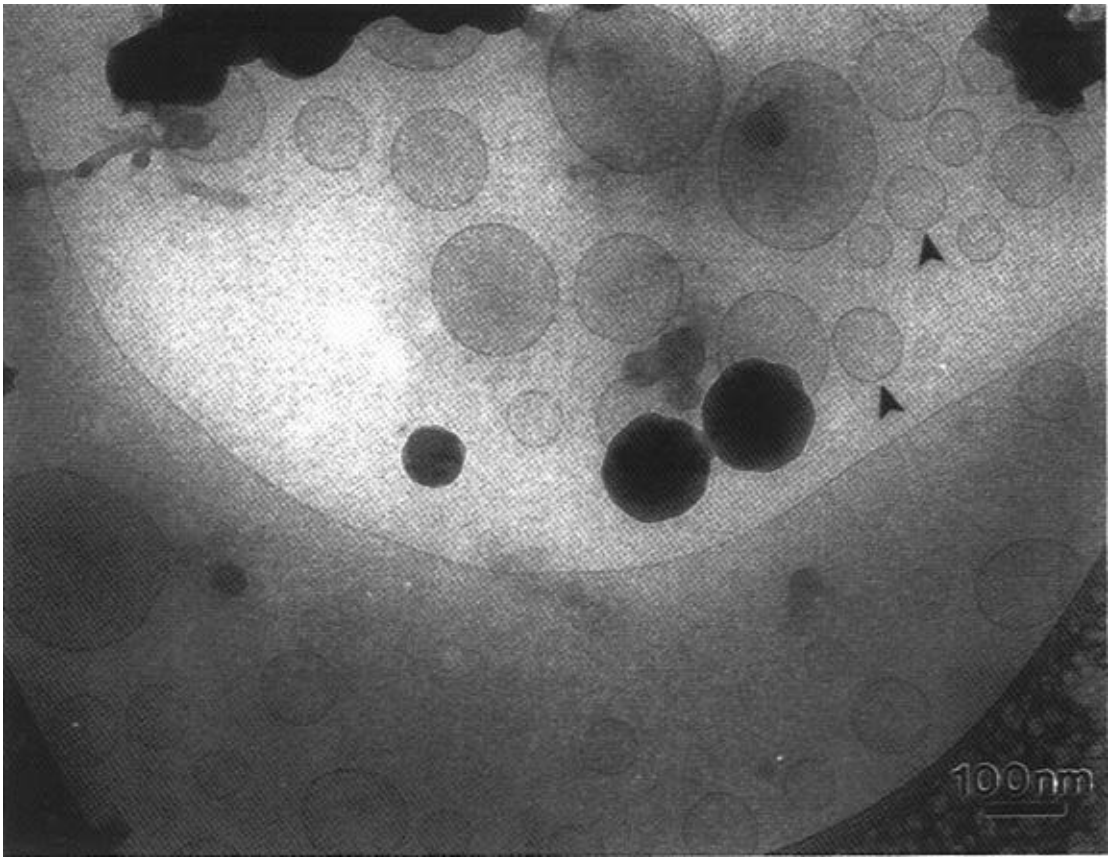

Figure 6. Cryoelectron micrograph showing well-formed spherical vesicles from the bottom phase of a two-phase sample at 4.57 wt % surfactant and a mixing ratio 80/20 CTAB to SOS.

5 is an electron micrograph of vesicles from a sample at 0.5 wt % surfactant. This dilute sample shows only large unilamellar vesicles of radius varying from 100 to 150 nm. Note that the bilayers appear flexible and the vesicles are not spherical. Such shapes may be the equilibrium conformations of vesicles because of the low bending rigidity of mixed bilayers,[17−19] or they may reflect deformations due to shear during sample preparation. The radii of the vesicles imaged are in good agreement with those measured with QLS (ca. 93 nm).

In CTAB-rich samples, a two-phase region separates the micelle and vesicle phases. Figure 6 shows a micrograph of the bottom (clear) phase of a two-phase sample at 4.57 wt % surfactant and a mixing ratio of CTAB/ SOS of 80/20. Spherical unilamellar vesicles with well-formed bilayers, approximately 100−300 nm in diameter, are present in this sample. In contrast to the SOS-rich vesicles, the bilayers are mostly spherical and do not appear to be deformed by shear. The top (viscous) phase (not shown) appears to contain a highly interconnected network of threadlike micelles.

Discussion

Phase behavior and microstructure in mixtures of oppositely charged surfactants are influenced greatly by the relative sizes of the hydrophobic portions of the surfactant molecules. Mixtures with unequal tail lengths promote the formation of vesicles relative to either multilamellar structures or the crystalline precipitate. When tail lengths are equal, as in mixtures of DTAB and SDS,[4] large polydisperse vesicles and multilamellar vesicles are formed, the vesicle phase is very narrow, and the crystalline precipitate forms over a wide range of compositions. In contrast, when the tail lengths of the two surfactants differ, as in the case presented here, the vesicle phase is considerably enlarged and precipitate is formed only at high dilution, or in equimolar mixtures. This likely represents the fact that the asymmetric tails cannot pack efficiently into a crystalline lattice, and so formation of precipitate is limited.

The limit of the vesicle phase at high surfactant concentration is set, at least approximately, by the close packing of vesicles. This concentration is generally only a few percent and is a function of the total surfactant concentration and surfactant solubility. Above this concentration, the surfactants form a multilamellar phase. Close packing will occur at lower concentrations if the vesicles are large, so vesicle phases at high surfactant concentration must contain small vesicles with highly curved bilayers. We have previously reported[3,11] that whenever the tail lengths of the two surfactants are not equal, the extent of the vesicle lobe is largest for mixtures rich in the shorter tailed (more soluble) surfactant, and this effect is obvious in Figure 1. Surfactant solubility is also important in setting the limit of vesicle stability because it determines the amount of surfactant in the form of aggregates for a given bulk composition. A relatively low surfactant solubility implies a large amount of aggregated surfactant and thus a high number density of vesicles.

The SOS-rich bilayers imaged in Figure 5 are apparently quite flexible, so the bending constant of these bilayers is low. Conversely, bilayers rich in CTAB (Figure 6) are considerably stiffer, and mostly spherical vesicles are observed. Theoretical calculations of the curvature elasticity of bilayers formed from single surfactants show that the bending energy of a bilayer is proportional to the length of the surfactant chain and ranges from ∼5 to 45 kT as the chain length increases from 8 to 16 carbons. Furthermore, the bending elastic constants are significantly reduced when short- and long-tailed surfactants are mixed.[18,19] This trend is supported by the apparent flexibility of the bilayers formed in mixtures of CTAB and SOS.

The micelle-to-vesicle phase transition is first order for

CTAB-rich mixtures and for SOS-rich mixtures at higher surfactant concentrations. At low surfactant concentrations there is limited micellar growth in SOS-rich mixtures and the transition occurs without phase separation. It is surprising that cryo-TEM micrographs show only small micelles, while QLS measurements indicate the presence of large aggregates in samples in the transition region (Figure 3, Table 1). This has also been reported for the solubilization of lipid membranes.[6,7,9,20−22] This phenomena is likely due to a low number density of vesicles in the sample. Light scattering is extremely sensitive to the largest particles in the solution; therefore, vesicles are detected even if they are very dilute. For a cryo-TEM experiment, on the other hand, a minute amount of solution is sampled, and the chances of this sample containing a statistically under-represented population are slim.

The time evolution of aggregate size, as followed by QLS, shows that the behavior of samples within the transition region is very different from that observed for samples with compositions well within the vesicle lobe. In particular, samples in the transition region have a high degree of polydispersity that increases with time and a poor signal-to-noise ratio that worsens with time. These observations are consistent with the presence of a heterogeneous size distribution, such as one with small aggregates contaminated with large polydisperse particles, that changes with time. The QLS results, combined with the observations of the presence of turbid clouds in samples within the transition region, provide strong support for the presence of large aggregates. Thus, we find that features of the transition observed in mixtures of oppositely charged surfactants are analogous to those observed for biological membranes.

The time scale for the transition from micelles to vesicles is much longer than that of the reverse transition from vesicles to micelles. Light-scattering experiments indicate that large aggregates are formed immediately after preparation of solutions that contain vesicles. However, the composition of the bilayer, and especially the partitioning of surfactant molecules between the inner and outer monolayers, plays an important role in setting the equilibrium bilayer curvature. It is well-established that a likely mode of adjusting these monolayer compositions, which is via surfactant flip-flop through the bilayer, occurs on time scales of up to days. These time scales are much longer than typical exchange rates of surfactant monomers between the aqueous and aggregated states, which is the only mass transfer mode necessary for micelles to equilibrate.

Surfactant degradation does not influence observations of the phase behavior and properties of aqueous mixtures of CTAB and SOS, provided that samples are made with properly purified SOS. Similar results hold for SDS.[16] The presence of octanol increases the turbidity of samples within the micelle/vesicle transition region and increases the amount and rate of growth of clouds in these samples.

These results also show the difficulty in assigning microstructure based on visual observations and light-scattering results alone, particularly in the region of the micelle/vesicle phase transition. In the two-phase samples, the vesicle phase ranges in appearance from clear and colorless to bluish and turbid, and in the SOS-rich samples, samples appear bluish, but apparently contain small micelles and a small population of large polydisperse aggregates. QLS can be used to discriminate between vesicles and this mixed population by examining the change of the apparent radius as a function of time. Vesicle samples have a relatively low polydispersity and attain an equilibrium size within several months, whereas the transition samples have a high degree of polydispersity that increases with time, and samples do not attain a reproducible equilibrium size even after 6 months.

Conclusion

Vesicles form in mixtures of oppositely charged surfactants with asymmetric chain lengths. The chain length asymmetry appears to stabilize vesicles relative to other microstructures, such as the liquid crystalline lamellar phase, as well as the crystalline precipitate. Further, we find that the bilayer properties are also determined by the composition; in particular, vesicles prepared with an excess of long-tailed surfactant are made of bilayers considerably stiffer than those rich in the short-tailed surfactant. As a result, important properties of the vesicles and the extent of the vesicle phase can be controlled with parameters that are experimentally accessible, such as surfactant geometry and composition.

The micelle-to-vesicle transition proceeds via a first-order phase transition for CTAB-rich mixtures and SOS-rich mixtures at higher surfactant concentrations. At lower concentrations, no phase separation is observed and the microstructure, determined from cryo-TEM observations, abruptly transforms from small spherical micelles to large unilamellar vesicles over a very narrow range of composition. Thus, we find that mixtures of oppositely charged surfactants exhibit many features similar to those observed in biological mixtures and may be a convenient model system for the investigation of phase behavior and morphology.

Acknowledgment. This work was supported by the National Science Foundation (CTS-9102719 and CTS-9319447). We are grateful to M. Bruche for performing NMR measurements.

References and Notes

(1) Kaler, E. W.; Herrington, K. L.; Miller, D. D.; Zasadzinski, J. A. In *Structure and Dynamics of Strongly Interacting Colloids and Supramolecular Aggregates in Solution*; Chen, S. H., Huang, J. S., Tartaglia, P., Eds.; Kluwer Academic Publishers: Dordrecht, The Netherlands, 1992; p 571.

(2) Kaler, E. W.; Murthy, A. K.; Rodriguez, B. E.; Zasadzinski, J. A. N. *Science* **1989**, *245*, 1371.

(3) Herrington, K. L. Phase Behavior and Microstructure in Aqueous Mixtures of Oppositely Charged Surfactants. Ph.D. Thesis, University of Delaware, 1994.

(4) Herrington, K. L.; Kaler, E. W.; Miller, D. D.; Zasadzinski, J. A.; Chiruvolu, S. *J. Phys. Chem.* **1993**, *97*, 13792.

(5) Almog, S.; Kushnir, T.; Nir, S.; Lichtenberg, D. *Biochemistry* **1986**, *25*, 2597.

(6) Kamenka, N.; Amrani, M. E.; Appell, J.; Lindheimer, M. *J. Colloid Interface Sci.* **1991**, *143*, 463.

(7) Ollivon, M.; Eidelman, O.; Blumenthal, R.; Walter, A. *Biochemistry* **1988**, *27*, 1695.

(8) Schurtenberger, P.; Mazer, N.; Känzig, W. *J. Phys. Chem.* **1985**, *89*, 1042.

(9) Vinson, P. K.; Talmon, Y.; Walter, A. *Biophys. J.* **1989**, *56*, 669.

(10) Kaler, E. W.; Herrington, K. L.; Murthy, A. K.; Zasadzinski, J. A. *J. Phys. Chem.* **1992**, *96*, 6698.

(11) Kaler, E. W.; Herrington, K. L.; Zasadzinski, J. A. N. In *Materials Research Society Symposia Proceedings, Complex Fluids*; Sirota, E. B., Weitz, D., Witten, T., Israelachvili, J., Eds.; Materials Research Society: Pittsburgh, 1991; Vol. 248, p 3.

(12) Rosen, M. J. *J. Colloid Interface Sci.* **1981**, *79*, 587.

(13) Reid, V. W.; Longman, G. F.; Heinerth, E. *Tenside* **1967**, *4*, 292.

(14) Koppel, D. E. *J. Chem. Phys.* **1972**, *57*, 4814.

(15) Bellare, J. R.; Davis, H. T.; Scriven, L. E.; Talmon, Y. *J. Electron Microsc. Tech.* **1988**, *10*, 87.

(16) Mysels, K. J. *Langmuir* **1986**, *2*, 423.

(17) Käs, J.; Sackmann, E. *Biophys. J.* **1991**, *60*, 825.

(18) Szleifer, I.; Kramer, D.; Ben-Shaul, A.; Gelbart, W. M.; Safran, S. A. *J. Chem. Phys.* **1990**, *92*, 6800.

(19) Szleifer, I.; Kramer, D.; Ben-Shaul, A.; Roux, D.; Gelbart, W. M. *Phys. Rev. Lett.* **1988**, *60*, 1966.

(20) Almog, S.; Litman, B. J.; Wimley, W.; Cohen, J.; Wachtel, E. J.; Barenholz, Y.; Ben-Shaul, A.; Lichtenberg, D. *Biochemistry* **1990**, *29*, 4582.

(21) Edwards, K.; Almgren, M.; Bellare, J.; Brown, W. *Langmuir* **1989**, *5*, 473.

(22) Egelhaaf, S. U.; Schurtenberger, P. *J. Phys. Chem.* **1994**, *98*, 8560.

JP952425R